SIMULATION AND EXPERIMENTAL CHARACTERIZATION OF THE BEARING BEHAVIOR OF CFRP-METAL LAMINATES

J. Both[1*], M. Wedekind[1], H. Baier[1]

[1]*Institute of Lightweight Structures, Department of Mechanical Engineering, Technical University of Munich, Boltzmannstraße 15, 85747 Garching bei München, Germany*
**both@llb.mw.tum.de*

Keywords: Fiber-metal laminate, bearing strength, in-situ effect, bolted joint

Abstract
The bearing behavior of CFRP-steel and CFRP-titanium laminates is characterized through finite element analysis (FEA) as well as experiments. The results are compared to the characteristics of pure CFRP laminates. This paper shows that bearing strengths can be increased significantly by substituting single laminae of a multidirectional composite by thin metal sheets. Steel layers show a higher potential by means of maximum load transfer but disadvantages considering weight aspects.

1 Introduction

Despite the advantages of carbon fiber reinforced plastics (CFRP, i.e. high specific strength, stiffness), there are still challenges to overcome when designing CFRP components. One challenge is the low bearing strength of unidirectional (UD) laminates. Reducing the fraction of UD 0° layers in a laminate will increase the bearing strength but will decrease the stiffness and tensile strength in loading direction significantly. Laminates with a quasi-isotropic layup show comparatively high bearing strengths but are still far inferior to metals. One approach to face this problem is to build up laminates consisting of both FRP and metallic layers. This hybridization may be performed directly at the load application area where single FRP layers are substituted by high strength steel or titanium layers [1, 2]. Hence a large share of UD 0° layers may still be maintained while guaranteeing sufficient bearing strength. Figure 1 shows the three different zones of such hybridized laminate. Experiments as well as simulations show that delaminations between laminae and metal layers in the transition zone, which are dominated by mode II, occur after failure of the laminate by bearing loading [3]. Therefore, in this research the focus is on the hybridized zone only.

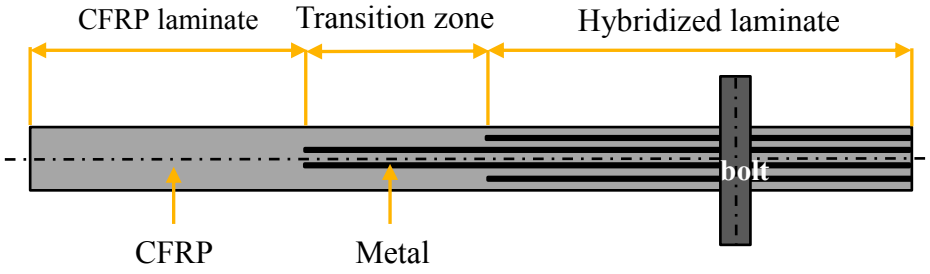

Figure 1. different zones of a hybridized laminate

The simulation of bolt or rivet joints requires high computational effort when utilizing 3D elements and contact boundary conditions. Instead an external force is applied to the laminate in this research, which replaces the bolts' mechanical influence on the laminate.

2 Materials and testing methods

2.1 Material properties

The CFRP used is an UD prepreg distributed by Advanced Composite Group of the United Kingdom consisting of the hot curing (180 °C) toughened epoxy resin MTM 44-1 and intermediate modulus carbon fibers IMS 65 by Tenax. The sheet metals used are both cold rolled. High strength steel X12CrNi177 (1.4324.8) as well as high strength titanium Ti15V3Cr3Sn3Al (15-3-3-3) sheets are applied. The elastic properties of these materials are listed in Table 1. $E_{1,2}$ represents the Young's modulus in and perpendicular to fiber direction, ν_{12} the Poisson's ratio, G_{12} the shear modulus and $\alpha_{1,2}$ the coefficients of thermal expansion (CTE) in corresponding directions. For both metals, the subscripts denote properties in (*1*) and perpendicular (*2*) to the rolling direction of the metals.

Material	**E_1 [GPa]**	**E_2 [GPa]**	**ν_{12} [-]**	**G_{12} [GPa]**	**α_1 [10^{-6}/K]**	**α_2 [10^{-6}/K]**
CFRP	175.9	8.1	0.32	4.4	-0.07	30.9
Steel	179.0	203.6	0.27	75.3*	14.8	15.0
Titanium	83.1	91.4	0.33	32.9*	8.2	9.1
*estimation						

Table 1. Elastic material properties

The ultimate strengths of all utilized materials are listed in Table 2. R_1^+ describes the ultimate tensile strength in fiber direction of an UD layer, R_1^- the compressive strength. R_{12} is the shear strength. In case of the metals, ultimate tensile strengths in and normal to the rolling direction are listed. It is assumed, that tensile and compression strengths of the metals are equal.

Material	**R_1^+ [MPa]**	**R_2^+ [MPa]**	**R_{12} [MPa]**	**R_1^- [MPa]**	**R_2^- [MPa]**
CFRP	3,289	55.9	73.1	1,595*	193*
Steel	1,532	1,548	--	1,532	1,548
Titanium	1,036	1,083	--	1,036	1,083
*estimation					

Table 2. Ultimate Strengths

The stresses at a plastic deformation of 0.2 % of the metals are listed in Table 3.

Material	**$R_{p0.2,1}^+$ [MPa]**	**$R_{p0.2,2}^+$ [MPa]**
Steel	1436.3	1385.8
Titanium	980.7	930.5

Table 3. stress values at a plastic deformation of 0.2 %

Figure 2 shows typical stress-strain graphs for the materials mentioned above.

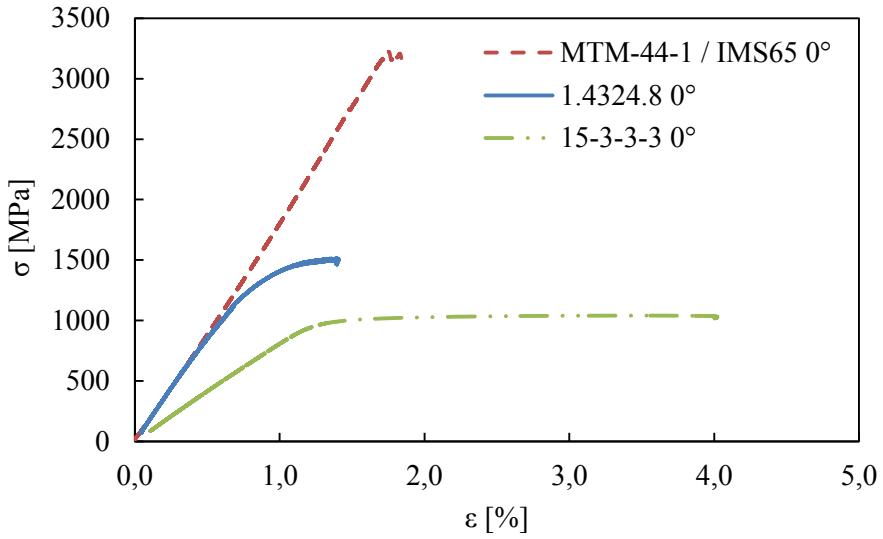

Figure 2. Stress-strain curves of CFRP (MTM-44-1 / IMS 65), steel (1.4324.8) and titanium (15-3-3-3) in fiber and rolling direction

2.2 Test setup

The tests to obtain the bearing strengths of CFRP and CFRP-metal laminates were carried out using the test-setup shown in Figure 3.

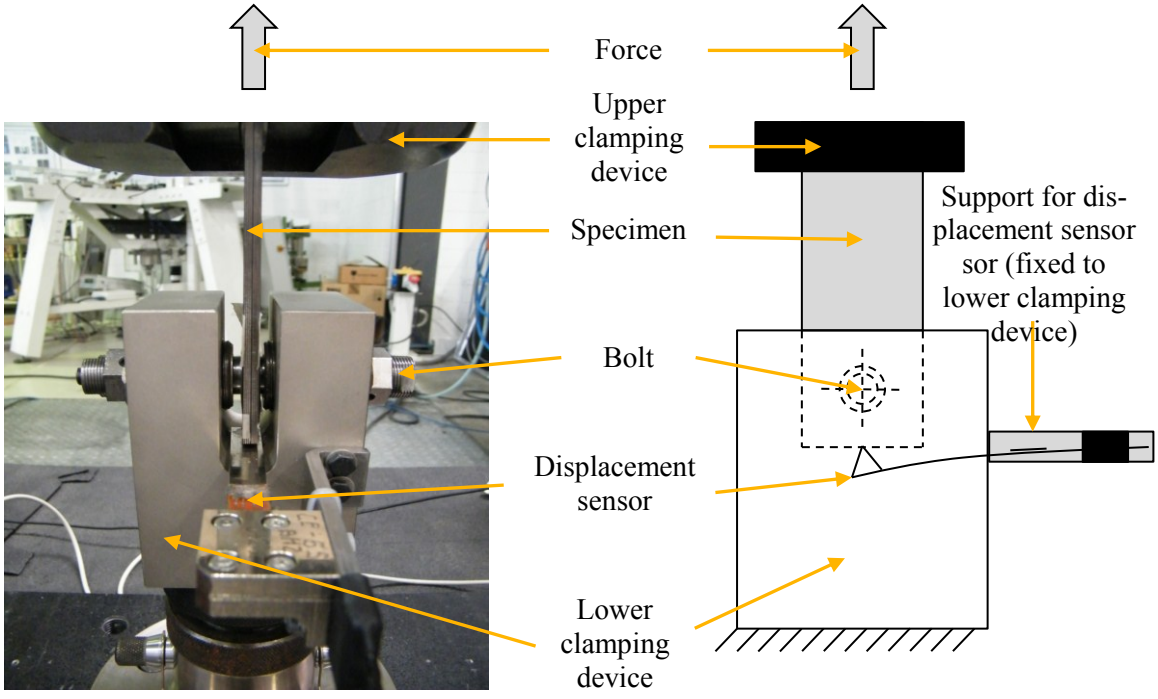

Figure 3. Left: Front view of test setup to determine bearing strengths; Right: Schematical side view

3 Results

3.1 Simulation details

The simulations were performed using the FEA program ANSYS (ANSYS Workbench in combination with ANSYS Composite Pre- and Post processing, ACP). The simulations were

performed using SHELL 181 elements. Figure 4 shows the modeling as well as an exemplary displacement in x-direction for one laminate configuration.

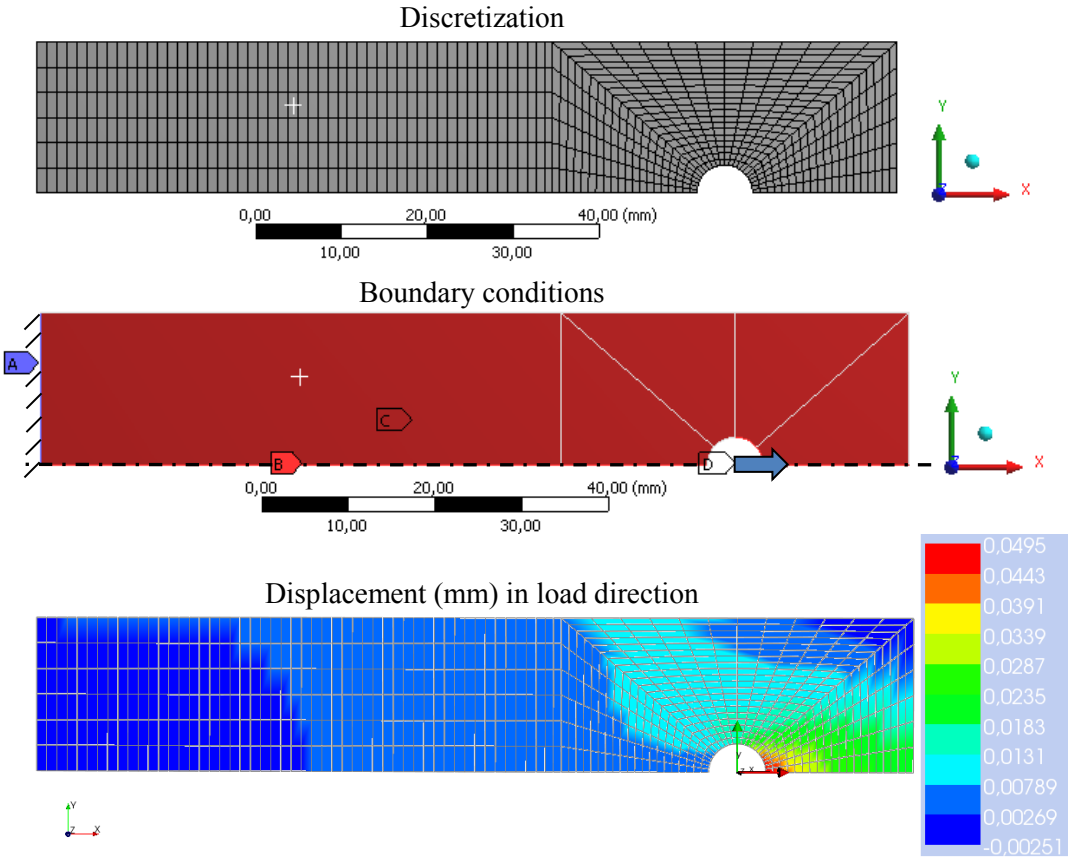

Figure 4. Top: finite element discretization, middle: boundary conditions: A: fixed support, B: symmetry plane, C: thermal load, D: external force acting on ¼ of the borehole, bottom: deformation in x-direction

For all simulations the in situ effect of embedded CFRP layers was accounted for. This effect considers a higher tensile strength normal to the fiber direction as well as a higher shear strength of a thin embedded layer in contrast to pure UD 90° and ±45° test results. According to [4], this effect may be quantified by equations 1 and 2:

$$R_2^{+,\text{in situ}} = \sqrt{\frac{8G_{Ic}}{\pi t \Lambda_{22}^0}} \tag{1}$$

$$R_{12}^{\text{in situ}} = \sqrt{\frac{8G_{IIc}}{\pi t \Lambda_{44}^0}} \tag{2}$$

with Λ_{22}^0 and Λ_{44}^0 according to equations (3) and (4):

$$\Lambda_{22}^0 = 2(\frac{1}{E_2} - \frac{\nu_{12}^2}{E_1}) \tag{3}$$

$$\Lambda_{44}^0 = \frac{1}{G_{12}} \tag{4}$$

The critical energy release rates G_{Ic} (delamination mode I) were determined through double cantilever beam (DCB) testing. The critical energy release rates G_{IIc} were estimated according to previously performed tests through end notched flexure (ENF) testing [3]. The in-situ strengths are listed in Table 4.

G_{Ic} [N/mm]	G_{IIc} [N/mm]	$R_2^{+,\text{in-situ}}$ [MPa]	$R_{12}^{\text{in-situ}}$ [MPa]
0.328	0.820	116.6	135.6

Table 4: Energy release rates and resulting in-situ strengths

As residual stresses arise below the glass transition temperature T_g, temperature loads ΔT are accounted for by the following relation:

$$\Delta T = \frac{1}{2}(T_{test} - T_{g,onset} - 20°C), \tag{5}$$

whereby $T_{g,onset}$ describes the temperature at the beginning of the glass transition interval (determined by differential scanning calorimetry, DSC) and T_{test} the test temperature at 23 °C. It is assumed that stresses are only able to build up at temperatures below $T_{g,onset}$ and that 50 % of the residual stresses relax after a certain time interval.

3.2. Simulation results

Figure 5 shows the effect of substituting CFRP plies by titanium or steel sheets on the onset of bearing failure for different laminate configurations. All laminates simulated have a symmetric layup and a total of 18 layers (total thickness 4.5 mm). The failure of the CFRP layers is determined by Cuntze's failure criterion [5], the onset of plasticization of the metal layers by the v. Mises criterion. The left laminate's layup is $[0/45/0/0/0/-45/0/90/0]_s$. Hence it contains 67 % 0° layers, 22 % 45° layers and 11% 90° layers ([67/22/11]). Every other layer, starting at the 45° layer is then substituted by titanium or steel sheets. Looking Figure 5, left, the critical layer is oriented at -45° to the loading direction which fails under compression loading in fiber direction (fc). After hybridization, plies oriented in loading direction are most likely to fail. It can be seen that the bearing stress at the onset of the failure of CFRP layers may be increased significantly by substituting plies by metal layers, but a plasticization of the metals takes place before fiber failure. Considering a laminate dominated by 45°-layers (layup: [0/45/-45/0/90/-45/45/90/0]), the bearing stress at the onset of bearing failure is increased only marginally by metal layers (see Figure 5, right).

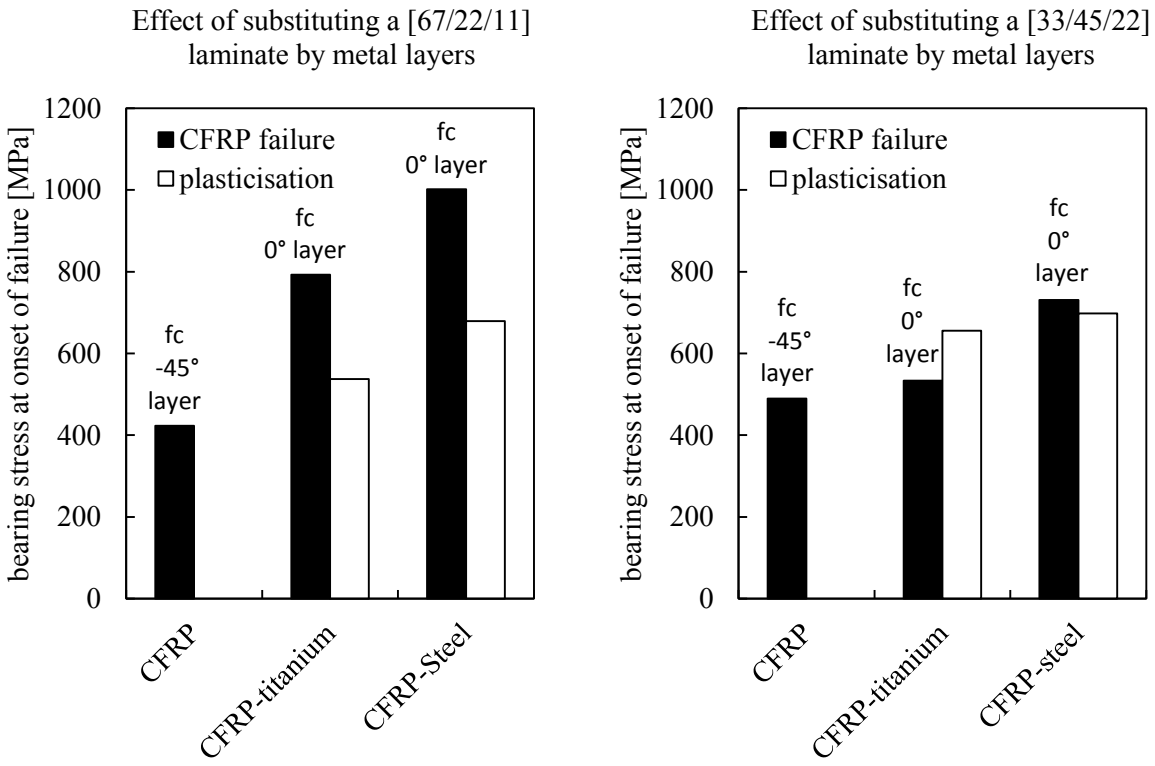

Figure 5. effect on the bearing stress at the onset of bearing failure through substituting CFRP-layers by metal layers: left: in a 0°-dominated laminate; right: in a (close to) quasi-isotropic layup

3.2. Comparison simulations – experiment

The simulations (see Figure 5, right) are compared to test results in Figure 6. As only linear elastic material models are used and no damage accumulation mechanisms are accounted for, a comparison is performed at the onset of a nonlinear behavior of the curve of the experiments. Simulation results are drawn into typical curve progressions of CFRP, CFRP-steel and CFRP-titanium specimens. Looking at the test results of CFRP specimens, the onset of bearing failure may be very well predicted with the chosen approach. In the case of hybrid specimens, the simulations underestimate the load bearing capability of these laminates. As the applied simulation approach shows conservative results it may nevertheless be used in order to pre-estimate the load bearing capability of hybrid laminates.

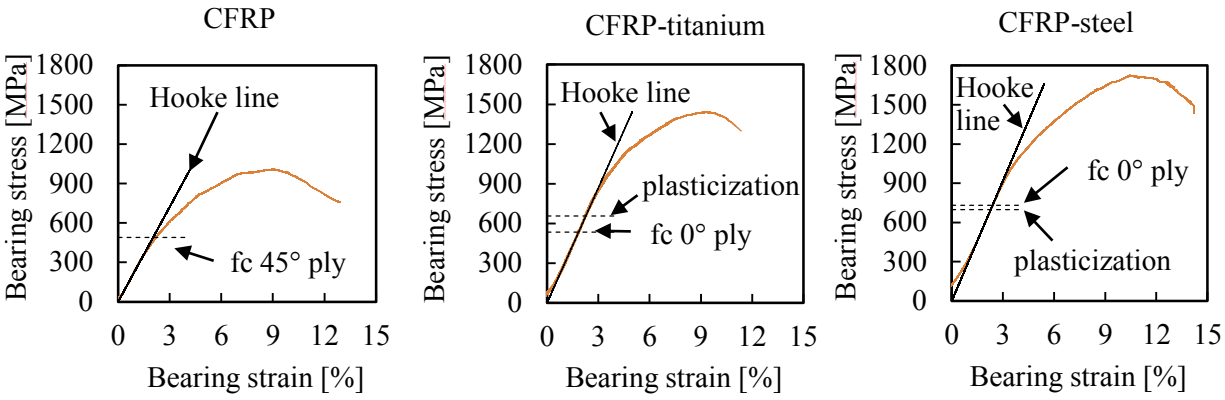

Figure 6. Comparison of test and simulation: left: pure CFRP specimens, middle: CFRP-titanium specimens; right: CFRP-steel specimens

A comparison of the tested laminate configurations with respect to bearing strengths at a borehole opening of 2 % and the ultimate bearing strengths are listed in Table 5. The weight specific values of CFRP are highest, followed by CFRP-titanium and CFRP-steel test results.

	Absolute values		Weight specific values	
Material	**2 % borehole opening [MPa]**	**Ultimate [MPa]**	**2 % borehole opening [10^3 (m/s)²]**	**Ultimate [10^3 (m/s)²]**
CFRP	846.2	988.6	564.1	659.1
CFRP-Titanium	1258.5	1556.0	444.2	549.2
CFRP-Steel	1450.7	1722.5	337.4	400.6

Table 5. absolute and weight specific bearing strengths of CFRP and hybrid CFRP-metal specimens

4 Conclusion and outlook

This paper shows a simulation approach as well as test results concerning the bearing behavior of CFRP, hybrid CFRP-titanium and CFRP-steel laminates. The onset of bearing failure of the CFRP specimens may be predicted with good accuracy, while the bearing behavior of hybrid laminates is underestimated by the chosen approach. Nevertheless, it was found that a hybridization is most effective considering laminates which show a high fraction of UD 0° layers in comparison to rather isotropic layups. Furthermore a hybridization should only be performed if the thickness of the load introduction area must be of similar thickness than the remaining part as weight specific bearing strengths are highest in pure CFRP laminates.

Acknowledgement
This work originates from the project "HyCoS - Hybrid Composite Structures" in cooperation with RUAG Aerospace and the German Aerospace Center (DLR) and is financed by the German Federal Ministry for Education and Research (Bundesministerium für Bildung und Forschung - BMBF).

References

[1] Camanho P., Fink A., Pimenta S., Obst A. *Hybrid composite laminates for high-performance bolted joints* in *Proceedings of ECCM 13*, Stockholm, Sweden, (2008).
[2] Hudley J., Yang J.-M., Hahn T., Facciano A. Bearing strength analysis of hybrid titanium composite laminates. *AIAA Journal*, **46**, pp. 2074-2085 (2008).
[3] Both J., Barfuß D., Baier H. *Mode II delamination of CFRP-metal laminates at bolted joints* in *Proceedings of ICCM 18*, Jeju Island, South Korea (2011).
[4] Dávila, C. G., Camanho P. P., Rose C. A. Failure Criteria for FRP Laminates. *Journal of Composite Materials*, **39 No. 4/2005**, pp. 323-345 (2005).
[5] Cuntze, R. Efficient 3D and 2D failure conditions for UD laminae and their application within the verification of the laminate design. *Composites Science and Technology,* **66** No. **7-8**, pp. 1081-1096 (2006)